Transition-density-fragment interaction combined with transfer integral approach for excitation-energy transfer via charge-transfer states

Fujimoto, Kazuhiro.J

Transition-density-fragment interaction combined with transfer integral approach for excitation-energy transfer via charge-transfer states

Kazuhiro J. Fujimoto

Citation: J. Chem. Phys. **137**, 034101 (2012); doi: 10.1063/1.4733669
View online: http://dx.doi.org/10.1063/1.4733669
View Table of Contents: http://jcp.aip.org/resource/1/JCPSA6/v137/i3
Published by the American Institute of Physics.

Transition-density-fragment interaction combined with transfer integral approach for excitation-energy transfer via charge-transfer states

Kazuhiro J. Fujimoto[a)]
Department of Computational Science, Graduate School of System Informatics, Kobe University, 1-1, Rokkodai, Nada, Kobe 657-850!, Japan

(Received 13 May 2012; accepted 21 June 2012; published online 16 July 2012)

A transition-density-fragment interaction (TDFI) combined with a transfer integral (TI) method is proposed. The TDFI method was previously developed for describing electronic Coulomb interaction, which was applied to excitation-energy transfer (EET) [K. J. Fujimoto and S. Hayashi, J. Am. Chem. Soc. **131**, 14152 (2009)] and exciton-coupled circular dichroism spectra [K. J. Fujimoto, J. Chem. Phys. **133**, 124101 (2010)]. In the present study, the TDFI method is extended to the exchange interaction, and hence it is combined with the TI method for applying to the EET via charge-transfer (CT) states. In this scheme, the overlap correction is also taken into account. To check the TDFI-TI accuracy, several test calculations are performed to an ethylene dimer. As a result, the TDFI-TI method gives a much improved description of the electronic coupling, compared with the previous TDFI method. Based on the successful description of the electronic coupling, the decomposition analysis is also performed with the TDFI-TI method. The present analysis clearly shows a large contribution from the Coulomb interaction in most of the cases, and a significant influence of the CT states at the small separation. In addition, the exchange interaction is found to be small in this system. The present approach is useful for analyzing and understanding the mechanism of EET. © *2012 American Institute of Physics*. [http://dx.doi.org/10.1063/1.4733669]

I. INTRODUCTION

Excitation-energy transfer (EET) is a well-known phenomenon observed in pairs or aggregates of molecules,[1,2] and its feature is widely used in biological systems such as green-plant photosynthesis.[3,4] In light-harvesting complex, sunlight energy captured by photosynthetic pigments is transferred to reaction center using EET.[5–7] The fundamental understanding of EET in biological system is expected to lead to more efficient artificial solar cells.[8] In the field of bioimaging, the EET process is usually called as fluorescent resonance energy transfer (FRET).[9] With the development of novel fluorescence probes, such as green fluorescent protein and quantum dots, the FRET technique has opened up new possibilities for visualizing the dynamics of biological process.[10] In recent years, the FRET analysis has been widely applied to protein-protein interactions in living cells.[11]

To clarify the EET mechanism, many theoretical studies were performed so far.[1,2] As a pioneering study, Förster derived the rate constant of EET using Fermi's golden rule.[12,13] In the framework of the Förster theory, an electronic coupling required for the EET rate is reduced to the Coulomb coupling termed as "pseudo Coulombic interaction," and hence the coupling is approximated to the dipole-dipole (dd) interaction using the transition dipole moments for individual chromophores. The dd method has been applied to various EET studies, because of its practical usefulness. In 1953, Dexter proposed a new type of EET mechanism, which is based on the electronic exchange interaction between two chromophores.[14] Owing to the exchange interaction, the Dexter mechanism works not only on the singlet-singlet transfer but also on the triplet-triplet transfer.[15] In common, the Dexter theory is considered to have an effect on the EET process at close separation of two chromophores.[10,15] In 1994, Harcourt *et al.* presented a significant influence of charge-transfer (CT) states on the EET process, on the basis of the perturbation treatment.[16] In their theory, the electronic coupling was described with two kinds of configurations. One is the local excitations within a chromophore, and the other is the CT states between two chromophores. Since the Förster and Dexter theories were based only on the local excitations, the admixture of the CT states provided a general framework for the electronic coupling. This EET incorporates a two-electron transfer (2ET) process, so that it is called as "2ET-assisted EET."[1] Figure 1 shows a schematic illustration for this process.

Since the electronic coupling has a strong influence on the EET rate, the accurate description of the electronic coupling has a significant role in the EET study. To this end, several methods have been proposed in the past.[17–33] The transition-density-fragment interaction (TDFI) method was developed also for this purpose.[34,35] Although the basic idea of TDFI is similar to that of the transition density cube (TDC) method proposed by Krueger *et al.*,[20] the transition densities used in TDFI are different from those in the TDC method. In the TDFI method, a self-consist procedure[36] is performed to the transition densities,[35] while the TDC method uses the transition densities calculated in gas-phase. In the previous studies, the TDFI calculations were applied to the EET process from salinixanthin (donor) to retinal (acceptor) chromophores in xanthorhodopsin,[34] and to an exciton-coupled circular dichroism spectrum observed in a dimerized retinal

a)Electronic mail: fujimoto@ruby.kobe-u.ac.jp

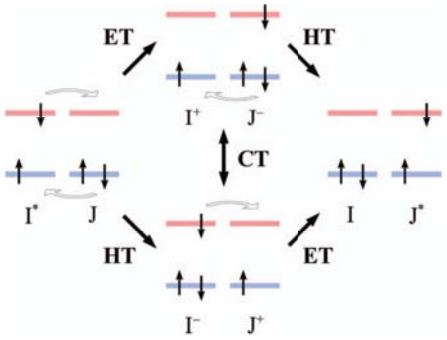

FIG. 1. Schematic illustration of the EET via CT states (2ET-assisted EET). Blue and red lines show the HOMO and LUMO of the monomer (I or J), respectively.

chromophore.[35] As a result, TDFI succeeded in quantitatively reproducing the experimental value of the electronic coupling, whereas the conventional dd method completely failed in describing the value.

The present study attempts to extend the TDFI method in three ways. First, the exchange interaction is included in the TDFI scheme. Since the previous TDFI method was restricted only to the Coulomb interaction, the description of the exchange interaction enables us to examine the Dexter mechanism. Second, the TDFI method is combined with the transfer integral (TI) approach[37] for taking into account the mixing of the CT states. Third, the overlap correction is applied to the electronic coupling energies. In this paper, the present approach is called as the TDFI-TI method. To check the accuracy of the TDFI-TI method, several test calculations are performed to an ethylene dimer. Based on the successful description of the electronic coupling, the energy components are also analyzed with the TDFI-TI method.

II. THEORY

A. The transition-density-fragment interaction (TDFI) method

The TDFI method was developed for calculating Coulomb interaction.[34,35] Compared with the previous study, the present TDFI method includes new features related to the description of exchange interaction and the overlap correction.

First, let us consider the total Hamiltonian for N molecules given by

$$\hat{H} = \sum_{I}^{N} \hat{H}_I + \sum_{I}^{N} \sum_{J>I}^{N} \hat{V}_{IJ}, \tag{1}$$

and the basis functions

$$|\Phi_1\rangle = \left|\Psi_I^{\mathrm{e}} \cdot \Psi_J^{\mathrm{g}}\right\rangle, \tag{2}$$

$$|\Phi_2\rangle = \left|\Psi_I^{\mathrm{g}} \cdot \Psi_J^{\mathrm{e}}\right\rangle. \tag{3}$$

In Eq. (1), $\hat{H}_I$ is the local Hamiltonian for the molecule I and $\hat{V}_{IJ}$ is the Coulomb interactions between the different molecules I and J. In Eqs. (2) and (3), Ψ_I^{g} and Ψ_J^{g} represent the ground states for the I and J molecules, respectively, and Ψ_I^{e} and Ψ_J^{e} are the excited states. For simplicity, only two molecules (i.e., $N = 2$) are concerned in this study.

Next, a one-electron transition density for the molecule X ($X = I$ or J) is introduced, which is defined by[38]

$$\begin{aligned}\rho_X^{\mathrm{eg}}(\mathbf{x}_1, \mathbf{x}'_1) \equiv N_{\mathrm{e}}^X \int \mathrm{d}\mathbf{x_2} \int \mathrm{d}\mathbf{x}_3 \ldots \\ \times \int \mathrm{d}\mathbf{x}_{N_{\mathrm{e}}} \Psi_X^{\mathrm{e}}(\mathbf{x}_1, \mathbf{x}_2, \mathbf{x}_3, \ldots, \mathbf{x}_{N_{\mathrm{e}}}) \\ \times \Psi_X^{\mathrm{g}\,*}(\mathbf{x}'_1, \mathbf{x}_2, \mathbf{x}_3, \ldots, \mathbf{x}_{N_{\mathrm{e}}}),\end{aligned} \tag{4}$$

where N_{e}^X denotes the number of electrons in the molecule X, and $\mathbf{x}_i$ expresses the space and spin coordinates of the i-th electron, i.e., $\mathbf{x}_i \equiv (\mathbf{r}_i, s_i)$. To obtain the spinless transition density, integration is performed over the spin coordinates s_1 and s'_1 as[38]

$$\rho_X^{\mathrm{eg}}(\mathbf{r}_1, \mathbf{r}'_1) = \int \mathrm{d}s_1 \int \mathrm{d}s'_1 \rho_X^{\mathrm{eg}}(\mathbf{x}_1, \mathbf{x}'_1). \tag{5}$$

Hereinafter, the spinless transition density, $\rho_X^{\mathrm{eg}}(\mathbf{r}_1, \mathbf{r}'_1)$, is just called the transition density.

Using the transition density, the off-diagonal Hamiltonian matrix element, $\langle\Phi_1|\,\hat{H}\,|\Phi_2\rangle$, is calculated as

$$\begin{aligned}\langle\Phi_1|\,\hat{H}\,|\Phi_2\rangle &= \langle\Phi_1|\,\hat{V}_{IJ}\,|\Phi_2\rangle \\ &= \int \mathrm{d}\mathbf{r}_1 \int \mathrm{d}\mathbf{r}'_1 \frac{\rho_I^{\mathrm{eg}*}(\mathbf{r}_1, \mathbf{r}_1)\rho_J^{\mathrm{eg}}(\mathbf{r}'_1, \mathbf{r}'_1)}{|\mathbf{r}_1 - \mathbf{r}'_1|} \\ &\quad -\frac{1}{2} \int \mathrm{d}\mathbf{r}_1 \int \mathrm{d}\mathbf{r}'_1 \frac{\rho_I^{\mathrm{eg}*}(\mathbf{r}_1, \mathbf{r}'_1)\rho_J^{\mathrm{eg}}(\mathbf{r}'_1, \mathbf{r}_1)}{|\mathbf{r}_1 - \mathbf{r}'_1|} \\ &\equiv V_{\mathrm{Coul}} + V_{\mathrm{Exch}},\end{aligned} \tag{6}$$

where the first and second terms correspond to the Coulomb and exchange interactions, respectively.

To convert Eq. (6) to a matrix form, the transition density by Eq. (5) is expanded in terms of atomic orbitals $\chi_\nu(\mathbf{r}_1)$ (AOs) as

$$\begin{aligned}&\rho_X^{\mathrm{eg}}(\mathbf{r}_1, \mathbf{r}'_1) \\ &= \sum_{\nu,\mu\in X} |\chi_\nu(\mathbf{r}_1)\rangle\, \langle\chi_\nu(\mathbf{r}_1)|\, \rho_X^{\mathrm{eg}}(\mathbf{r}_1, \mathbf{r}'_1)\, \left|\chi_\mu(\mathbf{r}'_1)\right\rangle \left\langle\chi_\mu(\mathbf{r}'_1)\right| \\ &= \sum_{\nu,\mu\in X} |\chi_\nu(\mathbf{r}_1)\rangle\, P_{\nu\mu}^X \left\langle\chi_\mu(\mathbf{r}'_1)\right|,\end{aligned} \tag{7}$$

with

$$P_{\nu\mu}^X = \langle\chi_\nu(\mathbf{r}_1)|\, \rho_X^{\mathrm{eg}}(\mathbf{r}_1, \mathbf{r}'_1)\, \left|\chi_\mu(\mathbf{r}'_1)\right\rangle. \tag{8}$$

Here, $P_{\nu\mu}^X$ is the transition density matrix of the molecule X in the AO representation. In the configuration interaction singles (CIS) method,[39] $P_{\nu\mu}^X$ is expressed by

$$P_{\nu\mu}^X = \sqrt{2} \sum_{a\in\mathrm{Vir.}} \sum_{i\in\mathrm{Occ.}} t_{i\to a}^X c_{\nu i}^X c_{a\mu}^X, \tag{9}$$

where $t_{i\to a}^X$ and $c_{\nu i}^X$ denote a configuration interaction (CI) coefficient and a linear combination of atomic orbital-molecular orbital (LCAO-MO) coefficient, respectively. Using Eq. (7),

Eq. (6) can be rewritten in the matrix form

$$\begin{aligned} V_{12}^0 &= \langle \Phi_1 | \hat{H} | \Phi_2 \rangle \\ &= \sum_{\nu,\mu\in I} \sum_{\lambda,\sigma\in J} P_{\nu\mu}^I P_{\lambda\sigma}^J \left[(\mu\nu|\sigma\lambda) - \frac{1}{2}(\mu\lambda|\sigma\nu) \right] \\ &\equiv V_{\mathrm{Coul}}^0 + V_{\mathrm{Exch}}^0, \end{aligned} \tag{10}$$

where

$$V_{\mathrm{Coul}}^0 = \sum_{\nu,\mu\in I} \sum_{\lambda,\sigma\in J} P_{\nu\mu}^I P_{\lambda\sigma}^J (\mu\nu|\sigma\lambda), \tag{11}$$

$$V_{\mathrm{Exch}}^0 = -\frac{1}{2} \sum_{\nu,\mu\in I} \sum_{\lambda,\sigma\in J} P_{\nu\mu}^I P_{\lambda\sigma}^J (\mu\lambda|\sigma\nu). \tag{12}$$

In Eqs. (10)–(12), $(\mu\nu|\sigma\lambda)$ expresses a two-electron integral in the AO representation, which is defined by

$$(\mu\nu|\sigma\lambda) \equiv \int \mathrm{d}\mathbf{r}_1 \int \mathrm{d}\mathbf{r}_2 \chi_\mu^*(\mathbf{r}_1)\chi_\nu(\mathbf{r}_1) r_{12}^{-1} \chi_\sigma^*(\mathbf{r}_2)\chi_\lambda(\mathbf{r}_2). \tag{13}$$

In my previous study, Eq. (11) was the TDFI expression for the Coulomb interaction, which is hold for the case that two basis functions shown in Eqs. (2) and (3) are orthogonal. If the orthogonality is not satisfied, the expressions of Eq. (10) is modified such as[37,40]

$$\begin{aligned} V^{\mathrm{TDFI}} &= \frac{1}{1-S_{12}^2} \left[V_{12}^0 - \frac{1}{2}(E_1+E_2) S_{12} \right] \\ &= \frac{V_{\mathrm{Coul}}^0}{1-S_{12}^2} + \frac{V_{\mathrm{Exch}}^0}{1-S_{12}^2} - \frac{(E_1+E_2) S_{12}}{2\left(1-S_{12}^2\right)}. \\ &\equiv V_{\mathrm{Coul}}^{\mathrm{TDFI}} + V_{\mathrm{Exch}}^{\mathrm{TDFI}} + V_{\mathrm{Ovlp}}^{\mathrm{TDFI}} \end{aligned} \tag{14}$$

To employ these forms, the overlap of two basis functions, S_{12}, and excitation energies for the I and J molecules, E_1 and E_2, are necessary. The overlap between the basis functions $|\Phi_1\rangle$ and $|\Phi_2\rangle$ is obtained from

$$\begin{aligned} S_{12} &= \langle \Phi_1 \mid \Phi_2 \rangle \\ &= -\frac{1}{N_{\mathrm{e}}^{IJ}} \sum_{\nu,\mu\in I} \sum_{\lambda,\sigma\in J} P_{\nu\mu}^I S_{\mu\lambda}^{\mathrm{AO}} P_{\lambda\sigma}^J S_{\sigma\nu}^{\mathrm{AO}}, \end{aligned} \tag{15}$$

where N_{e}^{IJ} is the number of electrons in the IJ complex and $S_{\mu\lambda}^{\mathrm{AO}}$ is an AO overlap matrix defined by

$$S_{\mu\lambda}^{\mathrm{AO}} \equiv \int \mathrm{d}\mathbf{r}_1 \chi_\mu^*(\mathbf{r}_1)\chi_\lambda(\mathbf{r}_1). \tag{16}$$

For the excitation energies, the polarization effects from the counterpart molecule are also taken into account, which leads to

$$\begin{aligned} E_1 &= \langle \Phi_1 | \hat{H} - E_0 | \Phi_1 \rangle \\ &= E_{\mathrm{ex}}^I + \sum_{\nu,\mu\in I} \left(P_{\nu\mu}^{I\mathrm{e}} - P_{\nu\mu}^{I\mathrm{g}} \right) \\ &\quad \times \left\{ V_{\mu\nu}^{\mathrm{nucl}J} + \sum_{\lambda,\sigma\in J} P_{\lambda\sigma}^{J\mathrm{g}} \left[(\mu\nu|\sigma\lambda) - \frac{1}{2}(\mu\lambda|\sigma\nu) \right] \right\}, \end{aligned} \tag{17}$$

$$\begin{aligned} E_2 &= \langle \Phi_2 | \hat{H} - E_0 | \Phi_2 \rangle \\ &= E_{\mathrm{ex}}^J + \sum_{\nu,\mu\in J} \left(P_{\nu\mu}^{J\mathrm{e}} - P_{\nu\mu}^{J\mathrm{g}} \right) \\ &\quad \times \left\{ V_{\mu\nu}^{\mathrm{nucl}I} + \sum_{\lambda,\sigma\in I} P_{\lambda\sigma}^{I\mathrm{g}} \left[(\mu\nu|\sigma\lambda) - \frac{1}{2}(\mu\lambda|\sigma\nu) \right] \right\}, \end{aligned} \tag{18}$$

where E_0 and E_{ex}^X denote the ground state energy of the IJ complex and the excitation energy of the noninteracting molecule X, respectively, and $V_{\mu\nu}^{\mathrm{nucl}X}$ expresses a nuclear potential generated by the molecule X which is defined by

$$V_{\mu\nu}^{\mathrm{nucl}X} \equiv \int \mathrm{d}\mathbf{r}_1 \chi_\mu^*(\mathbf{r}_1) \left[\sum_{A\in X}^{\mathrm{nucl}} \frac{-Z_A}{|\mathbf{r}_1 - \mathbf{R}_A|} \right] \chi_\nu(\mathbf{r}_1). \tag{19}$$

Here, Z_A and $\mathbf{R}_A$ denote the charge and the space coordinate of nucleus A, respectively. In Eqs. (17) and (18), $P_{\nu\mu}^{X\mathrm{g}}$ and $P_{\nu\mu}^{X\mathrm{e}}$ denote a one-electron density matrices (AO representation) of the molecule X in the ground and excited states, respectively. If the Hartree-Fock (HF)[41,42] and CIS methods are employed for describing the ground and excited states, respectively,[43] the ground state density matrix, $P_{\nu\mu}^{X\mathrm{g}}$, is represented by

$$P_{\nu\mu}^{X\mathrm{g}} = \sum_{i\in \mathrm{Occ.}} 2 c_{\nu i}^X c_{i\mu}^X, \tag{20}$$

and the excited state density matrix, $P_{\nu\mu}^{X\mathrm{e}}$, becomes

$$P_{\nu\mu}^{X\mathrm{e}} = \sum_{p,q} c_{\nu p}^X P_{pq}^{X\mathrm{e}} c_{q\mu}^X, \tag{21}$$

where

$$P_{pq}^{X\mathrm{e}} = \begin{cases} 2\delta_{pq} - \sum_{a\in \mathrm{Vir.}} t_{p\to a}^X t_{q\to a}^X & \text{if } p,q \in \mathrm{Occ.} \\ \sum_{i\in \mathrm{Occ.}} t_{i\to p}^X t_{i\to q}^X & \text{if } p,q \in \mathrm{Vir.} \\ 0 & \text{if others.} \end{cases} \tag{22}$$

Here, δ_{pq} is Kronecker delta. It should be noted that Eq. (21) means the molecular orbital (MO) to AO transformation of the excited state density matrix. To evaluate Eqs. (17) and (18), the density-fragment interaction (DFI) method[36] is employed. Using Eqs. (15) and (17), and (18), the overlap correction can be performed. In this study, Eq. (14) is the final expressions of TDFI for the Coulomb and exchange interactions.

B. The transfer integral (TI) method

In Sec. II A, the Coulomb and exchange interactions are considered, which correspond to the Förster[12] and Dexter[14] types of EET, respectively. In this section, a different type of EET, which is termed as the EET via CT states,[44] is concerned.

To account for the EET via CT states, the so-called TI,[37] which corresponds to the off-diagonal Hamiltonian matrix element, is required for describing the electron transfer (ET), hole transfer (HT), and CT processes. For this purpose, let us introduce two types of basis functions given by

$$|\Phi_3\rangle = \left| \Psi_I^+ \cdot \Psi_J^- \right\rangle, \tag{23}$$

$$|\Phi_4\rangle = \left|\Psi_I^- \cdot \Psi_J^+\right\rangle, \tag{24}$$

where Ψ_X^+ and Ψ_X^- represent the cationic and anionic states for the molecule X, respectively. Although many kinds of configurations can be selected to construct the basis functions, the present study restricts to the ones related only with highest occupied MO (HOMO) and lowest unoccupied MO (LUMO) of the molecules I and J, for simplicity.

First, let us consider the ET process. As shown in Fig. 1, the ET process is attributed to the LUMO-LUMO interaction between the molecules I and J.[17] In the ET process between $|\Phi_1\rangle$ and $|\Phi_3\rangle$, this interaction is expressed as

$$\begin{aligned} V_{\mathrm{ET1}}^0 &= \langle\Phi_1|\,\hat{H}\,|\Phi_3\rangle \\ &\simeq t_{\mathrm{H}\to\mathrm{L}}^I \left\{\langle\varphi_{\mathrm{L}}^I|\,\hat{F}\,|\varphi_{\mathrm{L}}^J\rangle + 2\left(\varphi_{\mathrm{L}}^I\varphi_{\mathrm{H}}^I\middle|\,\varphi_{\mathrm{H}}^I\varphi_{\mathrm{L}}^J\right) - \left(\varphi_{\mathrm{L}}^I\varphi_{\mathrm{L}}^J\middle|\,\varphi_{\mathrm{H}}^I\varphi_{\mathrm{H}}^I\right)\right\} \\ &= t_{\mathrm{H}\to\mathrm{L}}^I \left\{ \sum_{\alpha\in I}\sum_{\beta\in J} c_{\mathrm{L}\alpha}^I F_{\alpha\beta} c_{\beta\mathrm{L}}^J + \sum_{\mu\in I}\sum_{\nu\in I} c_{\nu\mathrm{H}}^I c_{\mathrm{L}\mu}^I \right. \\ &\quad \left. \times \sum_{\sigma\in I}\sum_{\lambda\in J} c_{\lambda\mathrm{L}}^J c_{\mathrm{H}\sigma}^I \left[2(\mu\nu|\sigma\lambda) - (\mu\lambda|\sigma\nu)\right] \right\}, \end{aligned} \tag{25}$$

where $\hat{F}$ is the Fock operator, and $F_{\mu\nu}$ is the Fock matrix in the AO representation

$$F_{\mu\nu} = h_{\mu\nu}^{\mathrm{core}} + \sum_{\sigma,\lambda}\sum_{k} 2c_{\lambda k}c_{k\sigma}\left[(\mu\nu|\sigma\lambda) - \frac{1}{2}(\mu\lambda|\sigma\nu)\right], \tag{26}$$

with the one-electron core Hamiltonian matrix

$$\begin{aligned} h_{\mu\nu}^{\mathrm{core}} &= \int \mathrm{d}\mathbf{r}_1 \chi_\mu^*(\mathbf{r}_1)\left[-\frac{1}{2}\nabla_1^2\right]\chi_\nu(\mathbf{r}_1) \\ &\quad + \int \mathrm{d}\mathbf{r}_1 \chi_\mu^*(\mathbf{r}_1)\left[\sum_A^{\mathrm{nucl}} \frac{-Z_A}{|\mathbf{r}_1 - \mathbf{R}_A|}\right]\chi_\nu(\mathbf{r}_1). \end{aligned} \tag{27}$$

In the second line of Eq. (25), the following definitions of MO integrals are used

$$\langle\varphi_i|\,\hat{F}\,|\varphi_i\rangle \equiv \int \mathrm{d}\mathbf{r}_1 \varphi_i^*(\mathbf{r}_1)\hat{F}\varphi_j(\mathbf{r}_1), \tag{28}$$

$$\left(\varphi_i\varphi_j\middle|\,\varphi_k\varphi_l\right) \equiv \int \mathrm{d}\mathbf{r}_1 \int \mathrm{d}\mathbf{r}_2 \varphi_i^*(\mathbf{r}_1)\varphi_j(\mathbf{r}_1) r_{12}^{-1} \varphi_k^*(\mathbf{r}_2)\varphi_l(\mathbf{r}_2). \tag{29}$$

In common cases of ET study, only LUMO-LUMO interaction is considered for evaluating TI of the ET process.[37] On the other hand, Eq. (25) contains an additional term $t_{\mathrm{H}\to\mathrm{L}}^I$ (i.e., the CI coefficient for the HOMO-LUMO transition in the molecule I) to account for the sequential process from the initial state $|\Phi_1\rangle$. A similar situation is also seen in the ET process between $|\Phi_4\rangle$ and $|\Phi_2\rangle$. In this case, $t_{\mathrm{H}\to\mathrm{L}}^I$ in Eq. (25) is replaced by $t_{\mathrm{H}\to\mathrm{L}}^J$ of the molecule J as follows:

$$\begin{aligned} V_{\mathrm{ET2}}^0 &= \langle\Phi_4|\,\hat{H}\,|\Phi_2\rangle \\ &\simeq t_{\mathrm{H}\to\mathrm{L}}^J \left\{\langle\varphi_{\mathrm{L}}^I|\,\hat{F}\,|\varphi_{\mathrm{L}}^J\rangle + 2\left(\varphi_{\mathrm{L}}^I\varphi_{\mathrm{H}}^J\middle|\,\varphi_{\mathrm{H}}^J\varphi_{\mathrm{L}}^J\right) - \left(\varphi_{\mathrm{L}}^I\varphi_{\mathrm{L}}^J\middle|\,\varphi_{\mathrm{H}}^J\varphi_{\mathrm{H}}^J\right)\right\} \\ &= t_{\mathrm{H}\to\mathrm{L}}^J \left\{ \sum_{\alpha\in I}\sum_{\beta\in J} c_{\mathrm{L}\alpha}^I F_{\alpha\beta} c_{\beta\mathrm{L}}^J + \sum_{\mu\in I}\sum_{\nu\in J} c_{\nu\mathrm{H}}^J c_{\mathrm{L}\mu}^I \right. \\ &\quad \left. \times \sum_{\sigma\in J}\sum_{\lambda\in J} c_{\lambda\mathrm{L}}^J c_{\mathrm{H}\sigma}^I \left[2(\mu\nu|\sigma\lambda) - (\mu\lambda|\sigma\nu)\right] \right\}. \end{aligned} \tag{30}$$

Second, the TI for the HT process is considered. As found from Fig. 1, the HT process is caused by the HOMO-HOMO interaction between the molecules I and J.[17] Therefore, it is calculated as

$$\begin{aligned} V_{\mathrm{HT1}}^0 &= \langle\Phi_1|\,\hat{H}\,|\Phi_4\rangle \\ &\simeq t_{\mathrm{H}\to\mathrm{L}}^I \left\{-\langle\varphi_{\mathrm{H}}^I|\,\hat{F}\,|\varphi_{\mathrm{H}}^J\rangle + 2\left(\varphi_{\mathrm{H}}^I\varphi_{\mathrm{L}}^J\middle|\,\varphi_{\mathrm{L}}^J\varphi_{\mathrm{H}}^J\right) - \left(\varphi_{\mathrm{H}}^I\varphi_{\mathrm{H}}^J\middle|\,\varphi_{\mathrm{L}}^J\varphi_{\mathrm{L}}^J\right)\right\} \\ &= t_{\mathrm{H}\to\mathrm{L}}^I \left\{ -\sum_{\alpha\in I}\sum_{\beta\in J} c_{\mathrm{H}\alpha}^I F_{\alpha\beta} c_{\beta\mathrm{H}}^J + \sum_{\mu\in I}\sum_{\nu\in I} c_{\nu\mathrm{L}}^I c_{\mathrm{H}\mu}^I \right. \\ &\quad \left. \times \sum_{\sigma\in J}\sum_{\lambda\in J} c_{\lambda\mathrm{H}}^J c_{\mathrm{L}\sigma}^J \left[2(\mu\nu|\sigma\lambda) - (\mu\lambda|\sigma\nu)\right] \right\}, \end{aligned} \tag{31}$$

$$\begin{aligned} V_{\mathrm{HT2}}^0 &= \langle\Phi_3|\,\hat{H}\,|\Phi_2\rangle \\ &\simeq t_{\mathrm{H}\to\mathrm{L}}^J \left\{-\langle\varphi_{\mathrm{H}}^I|\,\hat{F}\,|\varphi_{\mathrm{H}}^J\rangle + 2\left(\varphi_{\mathrm{H}}^I\varphi_{\mathrm{L}}^J\middle|\,\varphi_{\mathrm{L}}^J\varphi_{\mathrm{H}}^J\right) - \left(\varphi_{\mathrm{H}}^I\varphi_{\mathrm{H}}^J\middle|\,\varphi_{\mathrm{L}}^J\varphi_{\mathrm{L}}^J\right)\right\} \\ &= t_{\mathrm{H}\to\mathrm{L}}^J \left\{ -\sum_{\alpha\in I}\sum_{\beta\in J} c_{\mathrm{H}\alpha}^I F_{\alpha\beta} c_{\beta\mathrm{H}}^J + \sum_{\mu\in I}\sum_{\nu\in J} c_{\nu\mathrm{L}}^J c_{\mathrm{H}\mu}^I \right. \\ &\quad \left. \times \sum_{\sigma\in J}\sum_{\lambda\in J} c_{\lambda\mathrm{H}}^J c_{\mathrm{L}\sigma}^I \left[2(\mu\nu|\sigma\lambda) - (\mu\lambda|\sigma\nu)\right] \right\}. \end{aligned} \tag{32}$$

Similarly to Eqs. (25) and (30), Eqs. (31) and (32) have the CI coefficients, $t_{\mathrm{H}\to\mathrm{L}}^I$ and $t_{\mathrm{H}\to\mathrm{L}}^J$, respectively.

The third TI is involved in the CT process. As shown in Fig. 1, the CT process incorporates two kinds of interactions. One is the interactions between HOMO-LUMO and LUMO-HOMO for the molecules I and J, and the other is the HOMO-HOMO and LUMO-LUMO interactions. Thus, the TI for CT is expressed as follows:

$$\begin{aligned} V_{\mathrm{CT}}^0 &= \langle\Phi_3|\,\hat{H}\,|\Phi_4\rangle \\ &= 2\left(\varphi_{\mathrm{H}}^I\varphi_{\mathrm{L}}^J\middle|\,\varphi_{\mathrm{L}}^I\varphi_{\mathrm{H}}^J\right) - \left(\varphi_{\mathrm{H}}^I\varphi_{\mathrm{H}}^J\middle|\,\varphi_{\mathrm{L}}^I\varphi_{\mathrm{L}}^J\right) \\ &= \sum_{\mu\in I}\sum_{\nu\in J} c_{\nu\mathrm{L}}^J c_{\mathrm{H}\mu}^I \sum_{\sigma\in I}\sum_{\lambda\in J} c_{\lambda\mathrm{H}}^J c_{\mathrm{L}\sigma}^I \left[2(\mu\nu|\sigma\lambda) - (\mu\lambda|\sigma\nu)\right]. \end{aligned} \tag{33}$$

It should be noted that Eq. (33) has no contribution from $h_{\mu\nu}^{\mathrm{core}}$ because of the Slater-Condon rules.[45,46]

As mentioned in Sec. II A, the overlap correction is required also for TIs. The procedure is performed in the similar manner. In the ET, HT, and CT processes, the individual TIs are modified as

$$V_{\mathrm{ET1}} = \frac{1}{1 - S_{13}^2}\left[V_{\mathrm{ET1}}^0 - \frac{1}{2}(E_1 + E_2)\,S_{13}\right], \tag{34}$$

$$V_{\mathrm{HT1}} = \frac{1}{1 - S_{14}^2}\left[V_{\mathrm{HT1}}^0 - \frac{1}{2}(E_1 + E_2)\,S_{14}\right], \tag{35}$$

$$V_{\mathrm{CT}} = \frac{1}{1-S_{34}^2}\left[V_{\mathrm{CT}}^0 - \frac{1}{2}(E_1+E_2)\,S_{34}\right], \tag{36}$$

where S_{13}, S_{14}, and S_{34} are the overlaps between two basis functions, which are written as

$$S_{13} = \langle \Phi_1 \mid \Phi_3 \rangle \simeq -\frac{1}{N_{\mathrm{e}}^{IJ}} \sum_{\mu\in I}\sum_{\nu\in J} t^I_{\mathrm{H}\to\mathrm{L}} c^I_{\mathrm{L}\mu} S^{\mathrm{AO}}_{\mu\nu} c^J_{\nu\mathrm{L}}, \tag{37}$$

$$S_{14} = \langle \Phi_1 \mid \Phi_4 \rangle \simeq \frac{1}{N_{\mathrm{e}}^{IJ}} \sum_{\mu\in I}\sum_{\nu\in J} t^I_{\mathrm{H}\to\mathrm{L}} c^I_{\mathrm{H}\mu} S^{\mathrm{AO}}_{\mu\nu} c^J_{\nu\mathrm{H}}, \tag{38}$$

$$S_{34} = \langle \Phi_3 \mid \Phi_4 \rangle \simeq -\frac{1}{N_{\mathrm{e}}^{IJ}} \sum_{\mu,\sigma\in I}\sum_{\nu,\lambda\in J} c^J_{\nu\mathrm{L}} c^I_{\mathrm{H}\mu} S^{\mathrm{AO}}_{\mu\lambda} c^J_{\lambda\mathrm{H}} c^I_{\mathrm{L}\sigma} S^{\mathrm{AO}}_{\sigma\nu}. \tag{39}$$

To apply the correction to V^0_{ET2} and V^0_{HT2}, S_{13} and S_{14} used in Eqs. (34) and (35) are replaced by S_{42} and S_{32}, respectively, which give the overlap-corrected forms, V_{ET2} and V_{HT2}.

The Coulomb and exchange interactions (i.e., $V^{\mathrm{TDFI}}_{\mathrm{Coul}}$ and $V^{\mathrm{TDFI}}_{\mathrm{Exch}}$) shown in Sec. II A can be interpreted as the direct coupling between the states $|\Phi_1\rangle$ and $|\Phi_2\rangle$. On the other hand, the EET via CT states is to be the indirect one via the intermediate states $|\Phi_3\rangle$ and $|\Phi_4\rangle$. To express such an indirect coupling, the perturbation technique is often used for the electronic coupling,[37,47–49] which results in

$$\begin{aligned} T_{\mathrm{IF}} &= \langle\Phi_1|\hat{H}|\Phi_2\rangle + \left[-\frac{\langle\Phi_1|\hat{H}|\Phi_3\rangle\langle\Phi_3|\hat{H}|\Phi_2\rangle}{E_3-E_1} - \frac{\langle\Phi_1|\hat{H}|\Phi_4\rangle\langle\Phi_4|\hat{H}|\Phi_2\rangle}{E_4-E_1} \right. \\ &\quad \left. + \frac{\langle\Phi_1|\hat{H}|\Phi_3\rangle\langle\Phi_3|\hat{H}|\Phi_4\rangle\langle\Phi_4|\hat{H}|\Phi_2\rangle}{(E_3-E_1)(E_4-E_1)} + \frac{\langle\Phi_1|\hat{H}|\Phi_4\rangle\langle\Phi_4|\hat{H}|\Phi_3\rangle\langle\Phi_3|\hat{H}|\Phi_2\rangle}{(E_4-E_1)(E_3-E_1)} \right] \\ &\equiv T_{\mathrm{Direct}} + T_{\mathrm{Indirect}}, \end{aligned} \tag{40}$$

where the first term is the direct coupling, T_{Direct}, and the others is the indirect one, T_{Indirect}. Furthermore, substitution of the TIs for ET, HT, and CT into the corresponding Hamiltonian matrix elements in T_{Indirect} gives

$$\begin{aligned} T_{\mathrm{Indirect}} &= -\frac{V_{\mathrm{ET1}}V_{\mathrm{HT2}}}{E_3-E_1} - \frac{V_{\mathrm{HT1}}V_{\mathrm{ET2}}}{E_4-E_1} + \frac{V_{\mathrm{ET1}}V_{\mathrm{CT}}V_{\mathrm{ET2}}}{(E_3-E_1)(E_4-E_1)} \\ &\quad + \frac{V_{\mathrm{HT1}}V_{\mathrm{CT}}V_{\mathrm{HT2}}}{(E_4-E_1)(E_3-E_1)}. \end{aligned} \tag{41}$$

As found here, this form is similar to the superexchange coupling observed in the bridge-mediated EET (or ET),[1,28,37,47,50] while the intermediate states in Eq. (41) are not related to bridge molecules but to the IJ complex. In Eq. (41), the unknown terms are E_3 and E_4 corresponding to the energies of the charge-separated states. To calculate these values, ionization potential (IP), electron affinity (EA), and electron-hole attraction are necessary. For IP and EA, Koopmans' theorem[51] is employed, which are defined by[43]

$$E^X_{\mathrm{IP},i} \equiv {}^{N_{\mathrm{e}}^X-1}E^X_i - {}^{N_{\mathrm{e}}^X}E^X_0 \simeq -\varepsilon^X_i, \tag{42}$$

$$E^X_{\mathrm{EA},a} \equiv {}^{N_{\mathrm{e}}^X}E^X_0 - {}^{N_{\mathrm{e}}^X+1}E^X_a \simeq -\varepsilon^X_a, \tag{43}$$

where ε^X_i and ε^X_a are orbital energies of occupied orbital i and virtual orbital a for the molecule X, respectively. These orbital energies are also obtained with the DFI method for satisfying the self-consistency condition between the molecules I and J in the complex. For the electron-hole attraction, the HOMO-LUMO interaction between the molecules I and J is introduced as follows:

$$\begin{aligned} E^{+-}_{\mathrm{Coul}} &= -\left(\varphi^I_{\mathrm{H}}\varphi^I_{\mathrm{H}}\middle|\,\varphi^J_{\mathrm{L}}\varphi^J_{\mathrm{L}}\right) \\ &= -\sum_{\mu,\nu\in I}\sum_{\lambda,\sigma\in J} c^I_{\nu\mathrm{H}} c^I_{\mathrm{H}\mu} c^J_{\lambda\mathrm{L}} c^J_{\mathrm{L}\sigma} (\mu\nu|\sigma\lambda), \end{aligned} \tag{44}$$

$$\begin{aligned} E^{-+}_{\mathrm{Coul}} &= -\left(\varphi^I_{\mathrm{L}}\varphi^I_{\mathrm{L}}\middle|\,\varphi^J_{\mathrm{H}}\varphi^J_{\mathrm{H}}\right) \\ &= -\sum_{\mu,\nu\in I}\sum_{\lambda,\sigma\in J} c^I_{\nu\mathrm{L}} c^I_{\mathrm{L}\mu} c^J_{\lambda\mathrm{H}} c^J_{\mathrm{H}\sigma} (\mu\nu|\sigma\lambda), \end{aligned} \tag{45}$$

where E^{+-}_{Coul} (E^{-+}_{Coul}) denotes Coulomb interaction energies between a hole in HOMO for the molecule I (J) and an electron in LUMO for the molecule J (I).

According to Eqs. (42)–(45), E_3 and E_4 are calculated as

$$\begin{aligned} E_3 &= \langle\Phi_3|\hat{H} - E_0|\Phi_3\rangle \\ &\simeq E^I_{\mathrm{IP,H}} - E^J_{\mathrm{EA,L}} + E^{+-}_{\mathrm{Coul}} \\ &= -\varepsilon^I_{\mathrm{H}} + \varepsilon^J_{\mathrm{L}} - \sum_{\mu,\nu\in I}\sum_{\lambda,\sigma\in J} c^I_{\nu\mathrm{H}} c^I_{\mathrm{H}\mu} c^J_{\lambda\mathrm{L}} c^J_{\mathrm{L}\sigma} (\mu\nu|\sigma\lambda), \end{aligned} \tag{46}$$

$$\begin{aligned} E_4 &= \langle\Phi_4|\hat{H} - E_0|\Phi_4\rangle \\ &\simeq -E^I_{\mathrm{EA,L}} + E^J_{\mathrm{IP,H}} + E^{-+}_{\mathrm{Coul}} \\ &= \varepsilon^I_{\mathrm{L}} - \varepsilon^J_{\mathrm{H}} - \sum_{\mu,\nu\in I}\sum_{\lambda,\sigma\in J} c^I_{\nu\mathrm{L}} c^I_{\mathrm{L}\mu} c^J_{\lambda\mathrm{H}} c^J_{\mathrm{H}\sigma} (\mu\nu|\sigma\lambda). \end{aligned} \tag{47}$$

Finally, Eqs. (46) and (47) enable us to evaluate Eq. (41).

In this paper, the amount of the electronic coupling for EET is estimated by

$$T_{\mathrm{IF}} = T_{\mathrm{Direct}} + T_{\mathrm{Indirect}} = \left(V_{\mathrm{Coul}}^{\mathrm{TDFI}} + V_{\mathrm{Exch}}^{\mathrm{TDFI}} + V_{\mathrm{Ovlp}}^{\mathrm{TDFI}}\right) + \left(V^{\mathrm{TI(2)}} + V^{\mathrm{TI(3)}}\right), \quad (48)$$

where the TDFI expression by Eq. (14) is used in the direct coupling term, and the indirect coupling are separately described with the second and third order interactions with respect to TI, which are defined as follows

$$V^{\mathrm{TI(2)}} \equiv -\frac{V_{\mathrm{ET1}} V_{\mathrm{HT2}}}{E_3 - E_1} - \frac{V_{\mathrm{HT1}} V_{\mathrm{ET2}}}{E_4 - E_1}, \quad (49)$$

$$V^{\mathrm{TI(3)}} \equiv \frac{V_{\mathrm{ET1}} V_{\mathrm{CT}} V_{\mathrm{ET2}}}{(E_3 - E_1)(E_4 - E_1)} + \frac{V_{\mathrm{HT1}} V_{\mathrm{CT}} V_{\mathrm{HT2}}}{(E_4 - E_1)(E_3 - E_1)}. \quad (50)$$

III. COMPUTATIONAL DETAILS

In this study, the ethylene dimer was selected as a computational model. The atomic coordinate of this model was obtained from the geometry optimization using the second-order Møller-Plesset perturbation (MP2) theory[52] with the split valence double-ζ plus polarization basis set (6-31G*). This procedure was performed with the GAUSSIAN03 program package.[53] The optimized structure of the ethylene dimer is shown in Fig. 2(a). Using this structure, the TDFI-TI and full quantum-mechanical (QM) calculations were performed for testing the TDFI-TI accuracy.

In the excited state calculations, the CIS and time-dependent density functional theory (TD-DFT)[54,55] methods with a frozen core approximation to 1s core orbitals were employed for obtaining the excitation energies and the transition densities. In this process, the DFI algorithm[36] was used to satisfy the self-consistency condition between two molecules. It should be noted that although the present TDFI-TI method is derived from the wavefunction picture, the TDFI-TI calculation with TD-DFT is also performed. Recently, Pavanello and Neugebauer[56] proposed another type of the TI calculation with DFT, and they showed the significant influence of the self-interaction error (SIE)[57] on the electronic coupling. As mentioned in Sec. II B, the present TDFI-TI method uses Koopmans' theorem for the evaluations of IP and EA. Since the use of Koopmans' theorem in a DFT context is generally problematic also due to SIE,[58,59] the appropriate exchange-correlation functional is necessary. In this regard, the long-range corrected DFT is found to give the quantitative orbital energies.[60] Therefore, the revised Coulomb-attenuating method (rCAM) B3LYP functional[61] was used in the TD-DFT calculations. In this case, V_{Exch} in Eq. (6) was replaced by

$$V_{\mathrm{XC}} = c_{\mathrm{SR}}\left[-\frac{1}{2}\int \mathrm{d}\mathbf{r}_1 \int \mathrm{d}\mathbf{r}'_1 \frac{\rho_I^{\mathrm{eg}*}(\mathbf{r}_1, \mathbf{r}'_1)\rho_J^{\mathrm{eg}}(\mathbf{r}'_1, \mathbf{r}_1)}{|\mathbf{r}_1 - \mathbf{r}'_1|}\right] + c_{\mathrm{LR}}\left[-\frac{1}{2}\int \mathrm{d}\mathbf{r}_1 \int \mathrm{d}\mathbf{r}'_1 \frac{\rho_I^{\mathrm{eg}*}(\mathbf{r}_1, \mathbf{r}'_1)\mathrm{erf}(\mu|\mathbf{r}_1 - \mathbf{r}'_1|)\rho_J^{\mathrm{eg}}(\mathbf{r}'_1, \mathbf{r}_1)}{|\mathbf{r}_1 - \mathbf{r}'_1|}\right] + \int \mathrm{d}\mathbf{r}_1 \int \mathrm{d}\mathbf{r}'_1 \rho_I^{\mathrm{eg}*}(\mathbf{r}_1, \mathbf{r}_1) g_{\mathrm{XC}}(\mathbf{r}_1, \mathbf{r}'_1)\rho_J^{\mathrm{eg}}(\mathbf{r}'_1, \mathbf{r}'_1), \quad (51)$$

where $g_{\mathrm{XC}}(\mathbf{r}_1, \mathbf{r}'_1)$ stands for the exchange-correlation kernel, and c_{SR} and c_{LR} denote weights of the short-range and long-range HF exchange contributions, respectively.

The TDFI-TI program with CIS and TD-DFT was implemented in GAUSSIAN03.[53]

IV. RESULTS

A. Accuracy of the TDFI-TI method

For testing the TDFI-TI accuracy, the electronic coupling energies obtained with the TDFI-TI method were compared to those with the full-QM method. In the first step, the optimized structure of the ethylene dimer was used as the computational model.

In the full-QM calculations, the electronic coupling energies were evaluated with the so-called energy splitting in dimer (ESD) method,[37,62] which is defined by

$$\langle \Phi_1 | \hat{H} | \Phi_2 \rangle = \frac{1}{2}\left(E'_a - E'_b\right), \quad (52)$$

where E'_i denotes the i-th excited state energy for the dimer. Equation (52) strictly holds only for symmetric dimer with identical monomer energies.[22] To estimate the error associated with the TDFI-TI method, the value of Eq. (52) was taken as a reference, and the TDFI-TI value was compared with it. In both of the full-QM and TDFI-TI calculations, the CIS and TD-rCAM-B3LYP methods were employed to understand the dependence on the electronic structure method, as reported in previous studies.[63,64] As summarized in Table I, the TDFI-TI coupling energies obtained with CIS and

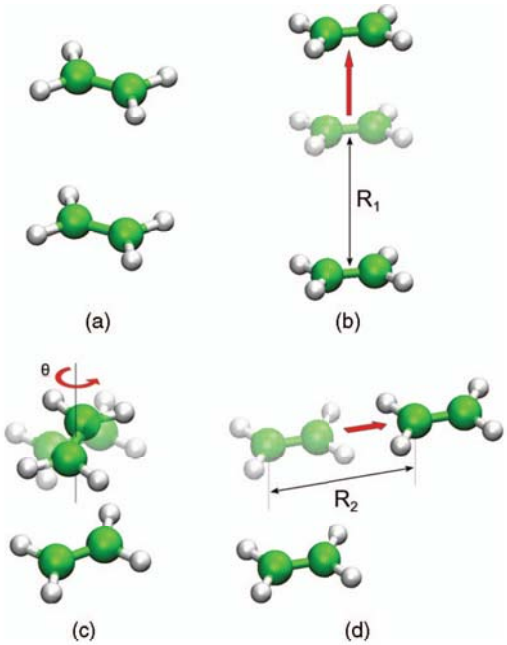

FIG. 2. (a) Optimized structure of the ethylene dimer. In (b-d), the definitions of x-axis coordinates for Figs. 3(a)–3(c) are shown.

TD-rCAM-B3LYP were to be 1997 and 1417 cm^{-1}, respectively, which indicates the absolute value of the coupling energy depends on the electronic structure method used in the TDFI-TI calculation (580 cm^{-1}). However, the TDFI-TI computations with CIS and TD-rCAM-B3LYP successfully reproduced the individual reference values (1976 and 1454 cm^{-1}) with the deviations of 21 and 37 cm^{-1}, respectively. Therefore, it is confirmed that TDFI-TI gives a quantitative value of the electronic coupling energy without regard to the electronic structure method used. Regarding the strong dependence of the electronic coupling on the electronic structure method, similar results were obtained in the previous study.[34,64] On the other hand, there are examples of linear-polyene type molecular dimers, for which pure and hybrid density functionals, CIS, and the semiempirical ZINDO/S methods give very similar couplings.[65,66] Therefore, it is considered that the dependence on the electronic structure method is system-dependent. This is an interesting topic, but the present study does not focus on it.

Table I also summarizes the coupling energies obtained with the previous TDFI method. As found here, the values of TDFI (CIS: 1649, TD-rCAM-B3LYP: 1097 cm^{-1}) were smaller than those of TDFI-TI. Therefore, the present TDFI-TI method was found to give a much improved description, compared with the previous TDFI method.

TABLE I. Electronic coupling energies of the ethylene dimer (cm^{-1}).

	CIS	TD-rCAM- B3LYP
Full QM	1976 (2079[a], 2039[b])	1454
TDFI-TI	1997 (2101[a], 2161[b])	1417
TDFI[c]	1649	1097

[a]Data calculated with the 6-31G basis set.
[b]Data calculated with the 6-311G** basis set.
[c]Previous TDFI method.[35]

To check the basis-set dependence, the TDFI-TI and full-QM calculations at the 6-31G and 6-311G** levels of basis sets were also performed. As listed in Table I, the TDFI-TI values calculated with 6-31G and 6-311G** were to be 2101 and 2161 cm^{-1}, respectively, while the full-QM ones were to be 2079 and 2039 cm^{-1}, respectively. From these results, the dependence on the basis set was found to be small in the present system (TDFI-TI: ∼164 cm^{-1} and full-QM: ∼103 cm^{-1}).

To obtain further insight into the TDFI-TI accuracy, I employed three kinds of computational models that differ with respect to the relative separation and orientation of the ethylene molecules. The schematic illustrations of these models are shown in Figs. 2(b)–2(d). Using these models, the electronic coupling energy calculations were performed with the TDFI-TI and full-QM methods. Figures 3(a)–3(c) show the evolutions of the electronic coupling energies as a function of the intermolecular distance, rotation, and translation, respectively. As found here, the TDFI-TI method reproduced almost the same values as the full-QM method in all the regions. The deviations from the reference values were to be ∼78 cm^{-1}, which were only ∼0.8% of the amount of the coupling energies. Therefore, the dependence on the relative separation and orientation was also confirmed to be small in the present TDFI-TI calculations.

B. Decomposition analysis of the electronic coupling energy

Based on the successful description of the electronic coupling energies, the contributions were analyzed in terms of five interactions (i.e., $V_{\mathrm{Coul}}^{\mathrm{TDFI}}$, $V_{\mathrm{Exch}}^{\mathrm{TDFI}}$, $V_{\mathrm{Ovlp}}^{\mathrm{TDFI}}$, $V^{\mathrm{TI}(2)}$, and $V^{\mathrm{TI}(3)}$ in Eq. (48)). The results are also shown in Figs. 3(a)–3(c). Here, it is noted that the decomposition analysis can be performed with the TDFI-TI method, not with the full-QM (ESD) method. This is one of the advantages of the TDFI-TI method. As shown in Figs. 3(a)–3(c), the Coulomb interaction predominantly contributed to the coupling energy in most of the regions calculated. In particular, it is visible at large separation in Fig. 3(a), where only the Coulomb interaction gives a contribution. On the other hand, the rest of the interactions showed a different behavior. As found in Fig. 3(a), the contributions from the indirect coupling (i.e., $V^{\mathrm{TI}(2)}$ and $V^{\mathrm{TI}(3)}$) gradually became large with the decrease in the molecular separation. At 3.0 Å, the values of the second order coupling $V^{\mathrm{TI}(2)}$ (5446 cm^{-1}) became larger than the Coulomb coupling energy (4689 cm^{-1}). Compared with the third order coupling $V^{\mathrm{TI}(3)}$, the second order coupling $V^{\mathrm{TI}(2)}$ was found to give a larger contribution, which means the two-step pathways through ET and HT are preferred to the three-step ones related to CT. This behavior was observed also in Figs. 3(b) and 3(c). Similarly to the indirect coupling, the exchange interaction contributed to the coupling energy at the small separation. However, the contribution was not as large as that from the indirect coupling, and hence the exchange interaction gave negative values (∼−943 cm^{-1}). Therefore, the

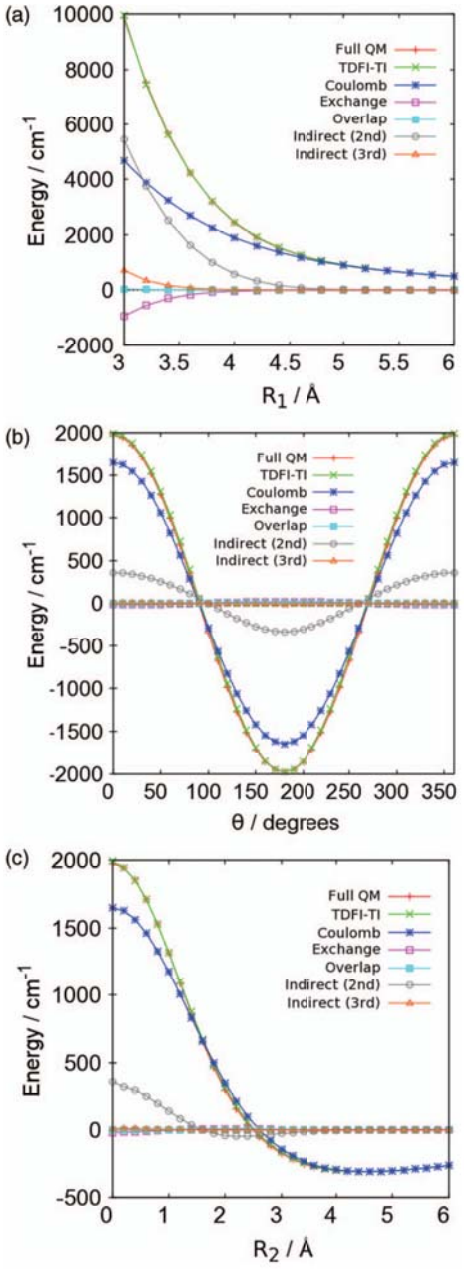

FIG. 3. Electronic coupling energies between two ethylene molecules as a function of (a) intermolecular distance, (b) rotation, and (c) translation. All calculations are performed with CIS/6-31G*.

amount of the coupling energy was found to be decreased by the exchange interaction. Although the exchange coupling is commonly considered as a main factor for EET at small separation, the indirect coupling had a larger contribution than the exchange coupling in the present system, as reported in previous study.[48] The overlap effect, $V_{\mathrm{Ovlp}}^{\mathrm{TDFI}}$, gave negligible contributions in all the cases ($\sim$40 cm^{-1}). From these results, it was found that the Coulomb interaction mainly contributes to the coupling energy in most of the cases, and the indirect coupling provides a significant contribution at the small separation. The present results also indicated that the calculation only of the Coulomb interaction is insufficient for the quantitative evaluation of electronic coupling energy.

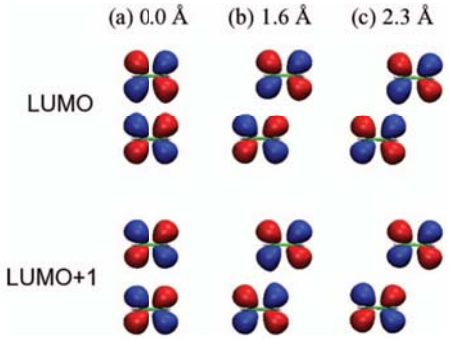

FIG. 4. The LUMOs and LUMO+1s of the ethylene dimer at (a) 0.0 Å, (b) 1.6 Å, and (c) 2.3 Å.

As found in Fig. 3(c), the curve of the second order coupling $V^{\mathrm{TI(2)}}$ showed a different shape from that of the total coupling energy. In particular, it provided negative values from more than 1.6 Å, and reached the minimum value at 2.3 Å (-48 cm^{-1}). To investigate this reason, the MOs of the ethylene dimer were analyzed, which are illustrated in Fig. 4. As a result, the LUMO and LUMO+1 at 0 and 2.3 Å had the bonding and anti-bonding characters, respectively. These two characters were easily distinguished. On the other hand, the characters of the LUMO and LUMO+1 at 1.6 Å could not be identified due to the mixing of bonding and anti-bonding characters. Since this mixing gives rise to the cancellation of the bonding and anti-bonding interactions, the electronic coupling becomes small as seen at 1.6 Å. Conversely, when the orbital characters are obviously identified, the electronic coupling becomes large because of their strong interactions. From these results, the magnitude of the second order coupling was found to be strongly related to the nodal characteristics of the orbital.

V. CONCLUSIONS

In this paper, the TDFI-TI approach for the EET via CT states was proposed. The basis of TDFI is to describe the electronic coupling between the transition densities for the individual molecules. Although the previous TDFI method was restricted to the electronic Coulomb interaction, the present TDFI was extended to the description of the exchange interaction. To apply to the EET via CT states, the TDFI method was also combined with the TI method, and hence the overlap correction was taken into account. As a result, the present TDFI-TI gave a much improved description of the electronic coupling, compared with the previous TDFI method. The TDFI-TI scheme can be combined with other electronic structure method, even though only the CIS and TD-rCAM-B3LYP methods were adopted in the present study. In addition, the decomposition analysis can be performed with the TDFI-TI method, which is convenient for investigating the main contribution of the electronic coupling energy.

In this study, the TDFI-TI method was applied to the ethylene dimer. As a result, it succeeded in quantitatively estimating the components of the coupling energy, whereas such an analysis could not be performed with the full-QM method. The present analysis clearly showed that the Coulomb

interaction mainly contributes to the coupling energy in most of the cases, and the indirect coupling provides a significant contribution at the small separation. Although the exchange coupling is commonly considered as a main factor for EET at small separation, the exchange coupling was smaller than the Coulomb and indirect couplings in the present system. These results supported the previous study by Scholes *et al.*[48] But it still remains unclear if the Dexter mechanism is effective or not, because the present results may hold only for the ethylene dimer. In this regard, further examinations are necessary for a better understanding of the EET mechanism. Such studies will be performed in my future work.

ACKNOWLEDGMENTS

This study was supported by a Grant-in-Aid for Scientific Research on Innovation Area, MEXT, Japan (23108709).

[1] V. May and O. Kühn, *Charge and Energy Transfer Dynamics in Molecular Systems* (Wiley-VCH, Weinheim, 2011).
[2] G. D. Scholes, Annu. Rev. Phys. Chem. **54**, 57 (2003).
[3] D. Beljonne, C. Curutchet, G. D. Scholes, and R. J. Silbey, J. Phys. Chem. B **113**, 6583 (2009).
[4] C. König and J. Neugebauer, ChemPhysChem **13**, 386 (2012).
[5] H. Sumi, Chem. Record **1**, 480 (2001).
[6] T. Ritz, A. Damjanović, and K. Schulten, ChemPhysChem **3**, 243 (2002).
[7] T. Renger, Photosynth. Res. **102**, 471 (2009).
[8] G. D. Scholes, G. R. Fleming, A. Olaya-Castro, and R. van Grondelle, Nat. Chem. **3**, 763 (2011).
[9] E. A. Jares-Erijman and T. M. Jovin, Nat. Biotechnol. **21**, 1387 (2003).
[10] M. Y. Berezin and S. Achilefu, Chem. Rev. **110**, 2641 (2010).
[11] A. Miyawaki, Dev. Cell **4**, 295 (2003).
[12] T. Förster, Ann. Phys. **437**, 55 (1948).
[13] T. Förster, in *Modern Quantum Chemistry*, edited by O. Sinanoğlu (Academic, New York, 1965), Vol. III, p. 93.
[14] D. L. Dexter, J. Chem. Phys. **21**, 836 (1953).
[15] S. Speiser, Chem. Rev. **96**, 1953 (1996).
[16] R. D. Harcourt, G. D. Scholes, and K. P. Ghiggino, J. Chem. Phys. **101**, 10521 (1994).
[17] A. Warshel and W. W. Parson, J. Am. Chem. Soc. **109**, 6143 (1987).
[18] H. Nagae, T. Kakitani, T. Katoh, and M. Mimuro, J. Chem. Phys. **98**, 8012 (1993).
[19] G. D. Scholes, K. P. Ghiggino, A. M. Oliver, and M. N. Paddon-Row, J. Phys. Chem. **97**, 11871 (1993).
[20] B. P. Krueger, G. D. Scholes, and G. R. Fleming, J. Phys. Chem. B **102**, 5378 (1998).
[21] A. Damjanović, T. Ritz, and K. Schulten, Phys. Rev. E **59**, 3293 (1999).
[22] S. Tretiak, C. Middleton, V. Chernyak, and S. Mukamel, J. Phys. Chem. B **104**, 4519 (2000).
[23] C.-P. Hsu, G. R. Fleming, M. Head-Gordon, and T. Head-Gordon, J. Chem. Phys. **114**, 3065 (2001).
[24] M. F. Iozzi, B. Mennucci, J. Tomasi, and R. Cammi, J. Chem. Phys. **120**, 7029 (2004).
[25] K. F. Wong, B. Bagchi, and P. J. Rossky, J. Phys. Chem. A **108**, 5752 (2004).
[26] M. E. Madjet, A. Abdurahman, and T. Renger, J. Phys. Chem. B **110**, 17268 (2006).
[27] J. Neugebauer, J. Chem. Phys. **126**, 134116 (2007).
[28] B. Fückel, A. Köhn, M. E. Harding, G. Diezemann, G. Hinze, T. Basché, and J. Gauss, J. Chem. Phys. **128**, 074505 (2008).
[29] R. F. Fink, J. Pfister, H. M. Zhao, and B. Engels, Chem. Phys. **346**, 275 (2008).
[30] H.-C. Chen, Z.-Q. You, and C.-P. Hsu, J. Chem. Phys. **129**, 084708 (2008).
[31] M. E. Madjet, F. Müh, and T. Renger, J. Phys. Chem. B **113**, 12603 (2009).
[32] S. Yeganeh and T. Van Voorhis, J. Phys. Chem. C **114**, 20756 (2010).
[33] T. Kawatsu, K. Matsuda, and J. Hasegawa, J. Phys. Chem. A **115**, 10814 (2011).
[34] K. J. Fujimoto and S. Hayashi, J. Am. Chem. Soc. **131**, 14152 (2009).
[35] K. J. Fujimoto, J. Chem. Phys. **133**, 124101 (2010).
[36] K. Fujimoto and W.-T. Yang, J. Chem. Phys. **129**, 054102 (2008).
[37] M. D. Newton, Chem. Rev. **91**, 767 (1991).
[38] R. McWeeny, Rev. Mod. Phys. **32**, 335 (1960).
[39] J. B. Foresman, M. Head-Gordon, J. A. Pople, and M. J. Frisch, J. Chem. Phys. **96**, 135 (1992).
[40] P.-O. Löwdin, J. Chem. Phys. **18**, 365 (1950).
[41] C. C. Roothaan, Rev. Mod. Phys. **23**, 69 (1951).
[42] G. G. Hall, Proc. R. Soc. London, Ser. A **205**, 541 (1951).
[43] T. Helgaker, P. Jørgensen, and J. Olsen, *Molecular Electronic-Structure Theory* (Wiley, Chichester, 2000).
[44] V. May, Dalton Trans. **45**, 10086 (2009).
[45] J. C. Slater, Phys. Rev. **34**, 1293 (1929).
[46] E. U. Condon, Phys. Rev. **36**, 1121 (1930).
[47] M. A. Ratner, J. Phys. Chem. **94**, 4877 (1990).
[48] G. D. Scholes, R. D. Harcourt, and K. P. Ghiggino, J. Chem. Phys. **102**, 9574 (1995).
[49] G. D. Scholes and R. D. Harcourt, J. Chem. Phys. **104**, 5054 (1996).
[50] C. Curutchet and B. Mennucci, J. Am. Chem. Soc. **127**, 16733 (2005).
[51] T. Koopmans, Physica **1**, 104 (1934).
[52] C. Møller and M. S. Plesset, Phys. Rev. **46**, 618 (1934).
[53] M. J. Frisch, G. W. Trucks, H. B. Schlegel *et al.*, GAUSSIAN03, Revision B.04, Gaussian, Inc., Pittsburgh, PA, 2003.
[54] E. Runge and E. K. U. Gross, Phys. Rev. Lett. **52**, 997 (1984).
[55] M. E. Casida, in *Recent Advances in Density Functional Methods*, Part I, edited by D. P. Chong (World Scientific, Singapore, 1995), p. 155.
[56] M. Pavanello and J. Neugebauer, J. Chem. Phys. **135**, 234103 (2011).
[57] J. P. Perdew and A. Zunger, Phys. Rev. B **23**, 5048 (1981).
[58] D. J. Tozer, J. Chem. Phys. **119**, 12697 (2003).
[59] O. Gritsenko and E. J. Baerends, J. Chem. Phys. **121**, 655 (2004).
[60] T. Tsuneda, J.-W. Song, S. Suzuki, and K. Hirao, J. Chem. Phys. **133**, 174101 (2010).
[61] A. J. Cohen, P. Mori-Sánchez, and W.-T. Yang, J. Chem. Phys. **126**, 191109 (2007).
[62] V. Coropceanu, J. Cornil, D. A. da Silva Filho, Y. Olivier, R. Silbey, and J.-L. Brédas, Chem. Rev. **107**, 926 (2007).
[63] A. Muñoz-Losa, C. Curutchet, I. Fdez. Galván, and B. Mennucci, J. Chem. Phys. **129**, 034104 (2008).
[64] E. Sagvolden, F. Furche, and A. Köhn, J. Chem. Theory Comput. **5**, 873 (2009).
[65] A. Strambi and B. Durbeej, J. Phys. Chem. B **113**, 5311 (2009).
[66] J. Neugebauer, J. Veldstra, and F. Buda, J. Phys. Chem. B **115**, 3216 (2011).